NMR Investigation of Segmental Dynamics in Disordered Styrene−Isoprene Tetrablock Copolymers

Yiyong He, T. R. Lutz, and M. D. Ediger*

Department of Chemistry, University of Wisconsin−Madison, Madison, Wisconsin 53706

Received June 23, 2003

ABSTRACT: ^{13}C and ^{2}H NMR relaxation time measurements were performed on four linear styrene−isoprene tetrablock copolymers (SISI) of overall molecular weight about 12 000 g/mol in order to characterize the segmental dynamics of both components. The two isoprene blocks are equal in length as are the two styrene blocks. A wide range of temperatures (from 285 to 530 K) and several compositions (volume fraction of styrene: 23%, 42%, 60%, and 80%) were investigated. Previous small-angle neutron scattering (SANS) results by Lodge et al. showed that these materials are homogeneous on length scales much larger than the radius of gyration. The segmental correlation times for both components in SISI were extracted by fitting the experimental data to the modified Kohlrausch−Williams−Watts (mKWW) orientation autocorrelation function and Vogel−Tammann−Fulcher (VTF) temperature dependence. While previous measurements found that the global dynamics in this system are quite homogeneous, these NMR measurements show that the segmental relaxation times of styrene and isoprene segments differ by orders of magnitude. At high temperatures, the dynamics of styrene segments are about 10 times slower than that of isoprene segments; this can be attributed to the difference in the intrinsic mobility of the two types of segments. The segmental dynamics of 5% polyisoprene (PI) tracers in one tetrablock matrix are very similar to that of the matrix isoprene segments.

Introduction

Miscible polymer mixtures are of great practical interest because mixing can lead to economical materials with desirable and tunable properties. Materials processing can also be facilitated by the modification of flow properties through blending. Unfortunately, the dynamics of miscible mixtures of chemically distinct polymers are significantly more complex[1−4] than those of homopolymer melts, making the prediction of miscible mixture rheology difficult. Time−temperature superposition fails in many miscible mixtures,[4,5] and the glass transitions of mixtures are typically much broader than the corresponding homopolymers.[1,6] The microscopic basis for these phenomena is that each component brings to the mixture a distinct dynamic behavior,[1,7] governed by its chemical structure and its local physical environment. Clearly it would be desirable to be able to predict the complex dynamic properties of mixtures based on homopolymer properties. A critical step toward this goal is to understand how the dynamics of each component change upon mixing.

Heterogeneity in segmental dynamics is generally accepted as a reasonable explanation for the complicated rheological behavior of miscible blends. Much effort has been made toward obtaining experimental information about segmental relaxation times for a variety of binary miscible blends, including polyisoprene/poly(vinyl ethylene) (PI/PVE),[1,4,7−16] polystyrene/poly(vinyl methyl ether) (PS/PVME),[17−20] poly(ethylene oxide)/poly(methyl methacrylate) (PEO/PMMA),[21−24] polystyrene/poly(2,6-dimethylphenylene oxide) (PS/PXE),[25,26] polystyrene/poly(tetramethyl carbonate) (PS/PTMC),[27,28] and poly(2-chlorostyrene)/poly(vinyl methyl ether) (P2CS/PVME).[29] It appears that in most cases the two components in miscible blends maintain distinct dynamics. The segmental relaxation times of the two components in a given blend can be different by many orders of magnitude even though the two types of chains are mixed at a molecular level.

Multiblock copolymers offer not only interesting morphological and material properties but also a new opportunity to test our understanding of dynamics in multicomponent systems. Tetrablocks of styrene and isoprene (SISI) have been studied from this point of view by Lodge and co-workers using small-angle neutron scattering (SANS), shear viscosity, and self-diffusion techniques.[30,31] SANS measurements indicate that these tetrablocks are homogeneous on length scales well beyond the radius of gyration.[30] A single effective monomeric friction coefficient $\zeta_{eff}(f_s,T)$ was extracted from viscosity measurements, whereas the individual friction factors ζ_{PS} and ζ_{PI} were obtained from tracer diffusion. A remarkable feature of these results was the fact that in a given matrix and at a given temperature, $\zeta_{eff} \approx \zeta_{PS} \approx \zeta_{PI}$. This result is surprising. The large ΔT_g of the homopolymers PS and PI, and some previous experimental work,[32] indicate that the segmental dynamics should be very heterogeneous in the tetrablocks. In miscible blend systems, heterogeneous segmental dynamics leads to tracer friction coefficients with distinct temperature and composition dependences. In an effort to understand why this is not the case in SISI tetrablocks, the characterization of the segmental dynamics for both isoprene and styrene components in this system over a wide temperature and composition range is presented here.

In this paper, NMR measurements were used to obtain ^{13}C T_1 (and NOE) and ^{2}H T_1 for the same SISI samples used in the work of Lodge and co-workers.[30,31] The styrene content for these samples ranges from 23% to 80%. A wide range of temperatures (280−530 K) was investigated at two magnetic fields. NMR methods based upon isotopic labeling provide a clean separation of component dynamics. For both components at each

* Author for correspondence: e-mail ediger@chem.wisc.edu.

10.1021/ma030350g CCC: $25.00
Published on Web 09/18/2003

Table 1. Characterization of Tetrablock Copolymers and Homopolymers

	block molecular weight (g/mol)					
samples	styrene	isoprene	styrene	isoprene	f_s[b]	T_g (K)
PI-1K		900				
PI-11K		10500				
PI		1350			0.00	201
SISI23[a]	1400	4400	1600	4400	0.23	228.9[c]
SISI42[a]	2600	3300	2900	3300	0.42	257.6[c]
SISI60[a]	3000	1900	3500	1900	0.60	294.1[c]
SISI80[a]	4900	1100	5200	1100	0.80	312.6[c]
PS	10900				1.00	366.7

[a] From ref 30. [b] Based on the styrene segment volume (ref 30). [c] Measured by rheology (ref 30).

composition, segmental correlation times were extracted by fitting T_1 (and NOE) data to the mKWW (modified KWW) autocorrelation function and the VTF temperature dependence. In addition, a NMR measurement on the segmental dynamics of ^{13}C-labeled PI tracer in one tetrablock matrix was performed in order to understand tracer dynamics in these systems.

The major conclusions of our study are as follows: (1) SISI tetrablock copolymers show strong segmental dynamic heterogeneity. The dynamic difference between the two components becomes larger at lower temperatures. (2) At sufficiently high temperatures, the segmental dynamics of styrene segments are slower than that of isoprene segments by about 1 decade. This can be explained by the intrinsic mobility difference between the two types of segments. (3) NMR measurements on ^{13}C-labeled PI tracer dissolved in the SISI60 matrix showed that the segmental dynamics of the PI tracer are almost identical to (but slightly faster than) those of isoprene segments in SISI. This is consistent with the influence of junction points on the dynamics of nearby segments.

The heterogeneity on the segmental level, in contrast to the approximate homogeneity on the global level, makes SISI tetrablocks very interesting mixtures. In a future paper, we consider the quantitative relationship between the segmental and global dynamics in this system.[33]

Experimental Section

Materials. Four SISI tetrablock copolymers of varying composition, synthesized through living anionic polymerization by Dr. Steve Smith,[30] were provided by Prof. Tim Lodge. Their structures are regular in the sense that the two styrene blocks have about the same length, as do the two isoprene blocks. The styrene units are a random mixture of 25% perdeuteriostyrene and 75% protiostyrene. The total degree of polymerization $N \approx 120$ is roughly the same in the four copolymers. Previous SANS measurements[30] showed that these materials are homogeneous on length scales larger than the radius of gyration even though styrene and isoprene interact unfavorably.[34,35] The order−disorder transition temperatures for all four samples are estimated to be below −50 °C and thus far from the temperature range of this study. Characterization information is shown in Table 1. The numerical suffixes in the sample codes SISI23, SISI42, SISI60, and SISI80 specify the styrene volume percentage f_s.

The molecular weights of all homopolymers are also listed in Table 1. PI, PI-1K, and PI-11K (with $M_w/M_n = 1.11$, 1.39, and 1.02, respectively) were synthesized by Dr. Marinos Pitsikalis. The details regarding the purification, synthesis, and characterization are available elsewhere.[16,36] Both PI-1K and PI-11K are ^{13}C-labeled samples with 66% ^{13}C enrichment for one methylene carbon (C1 in Figure 1). Perdeuterated d_8-PS (PS in Table 1) with $M_w/M_n = 1.05$ was purchased from Polymer Source Inc. (P903-dPS).

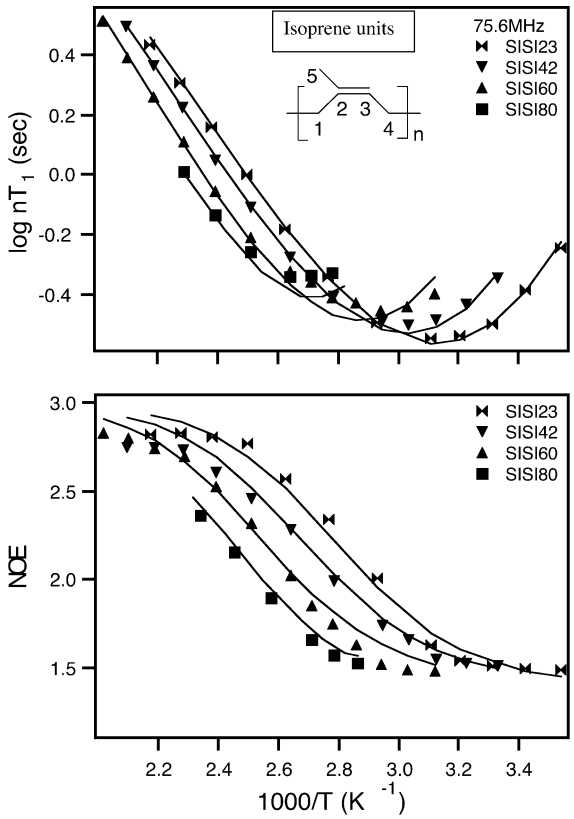

Figure 1. ^{13}C NMR relaxation time measurements for C1 carbons in isoprene segments of the four tetrablock copolymers at 75.6 MHz. Solid lines are the fit results using the mKWW autocorrelation function and VTF temperature dependence.

NMR Sample Preparation. SISI23 has the lowest T_g of the four copolymers. We dissolved it in cyclopentane to make a dilute solution and then transferred the solution to a NMR tube. About 90% of the solvent was removed under partial vacuum. The resulting concentrated solution was physically coated onto the wall of the NMR tube to make a layer less than 1 mm thick. Vacuum was then applied while holding the tube horizontally. After 72 h, the tube was sealed under vacuum and placed vertically in an oven at 50 °C for another hour to allow the sample to flow down to the bottom of the tube. From inspection of the ^{13}C NMR spectrum, no solvent remained at a level higher than 1%. Two more blends, containing either 5% PI-1K or 5% PI-11K in SISI60, were prepared in the same way. The blend of 5% PI-11K in SISI60 is only miscible at temperatures above 130 °C.

SISI42 and SISI60 could be easily cooled to below their T_g by placing them in a pan on dry ice. Solid granules were loaded into NMR tubes in cold CO_2 environment in order to prevent the condensation of water vapor. The NMR tubes were then placed on a vacuum line, warmed slowly to room temperature, and sealed after 12 h.

Pure PI is a low-viscosity liquid at ambient temperature and could be directly poured into NMR tubes; SISI80 and PS were loaded into NMR tubes as granular solids.

NMR Measurements. Two different relaxation measurements, spin−lattice relaxation time (T_1) and nuclear Overhauser effect (NOE), were conducted over a wide temperature range. Both NMR observables detect the segmental dynamics as they are sensitive to reorientation of C−H or C−D bond vectors. T_1 was measured by the standard $\pi-\tau-\pi/2$ pulse sequence, waiting at least $8T_1$ between the acquisition and the next pulse. NOE was measured as the ratio of ^{13}C signal intensity from the spectrum with continuous decoupling to that with inverse-gated decoupling, waiting at least $10T_1$ between acquisitions. The number of scans used for signal averaging

ranged from 8 to 64, depending on the sample and temperature. The measurements were performed on a Varian Inova-500 NMR spectrometer with a Doty high-temperature probe and a Bruker DMX-300 NMR spectrometer using a homemade probe. Spectra were processed with line broadening equal to one-tenth of the line width of the spectra. Temperature was controlled to ±0.5 K and calibrated to within an uncertainty of ±2 K using a combination of an ethylene glycol thermometer[37] and melting point standards.

In this work, we selectively measured ^{13}C and ^{2}H signals for isoprene and styrene units, respectively. In this way we could obtain the dynamic information for isoprene and styrene segments without interference from each other. For the isoprene component, ^{13}C T_1 and NOE experiments were performed on the two methylene carbons (C1 and C4 in Figure 1) from 285 to 500 K at ^{13}C Larmor frequencies of 75.6 and 125.2 MHz. For the styrene component, ^{2}H T_1 were measured for both backbone and phenyl ring deuterons from 330 to 530 K at ^{2}H Larmor frequencies of 46.1 and 76.8 MHz. At low temperatures substantial overlap was observed between the two kinds of deuterium resonance lines. Since the two kinds of deuterons have very similar T_1 values and very similar temperature dependences, to interpret the data consistently, we averaged the T_1 values over all eight deuterons for all temperatures and used these rate-averaged T_1 values in our analysis.

The following procedure was used to ensure that no temperature-induced degradation[38,39] took place during experiments. We first took NMR measurements on the isoprene units at low temperature. Additional experiments were performed from low to high temperature. Following the experiments at the highest temperature, repeated measurements were made on the isoprene units at two low temperatures. For each sample, T_1 and NOE agreed with the original measurements within the experimental uncertainty (±3%).

NMR Relaxation Equations. Depending on the nucleus and its chemical environment, there can be several contributions to the observed NMR relaxation rates, including dipolar interaction, chemical shift anisotropy, and quadrupolar relaxation.[40] Nuclear spin relaxation is caused by fluctuating local fields through these mechanisms. It is the orientational motion of internuclear vectors that causes such fluctuations, and to the extent that these fluctuations have frequency components at the resonance frequency for the nuclei of interest they will cause relaxation.

The quantitative connection between molecular motion and spin relaxation is made through the spectral density function, which is defined by

$$J(\omega) = {}^1/_2\int_{-\infty}^{\infty} G(t)\exp(-i\omega t)\,dt \tag{1}$$

Here $G(t)$ is the orientation autocorrelation function which describes the reorientation of the internuclear vector ($^{13}C-H$ or C−D in our experiments):

$$G(t) = \frac{3}{2}\langle\cos^2\theta(t)\rangle - \frac{1}{2} \tag{2}$$

Here $\theta(t)$ is the angle of a $^{13}C-H$ or C−D bond at time t relative to its original position. The brackets denote the ensemble average over a collection of nuclei. $J(\omega)$ expresses the power available at frequency ω to relax the spins in question.

For the methylene carbons of isoprene segments, the dipolar interaction is the dominant relaxation mechanism for $^{13}C-H$ bond relaxation, and ^{13}C T_1 and NOE are given by[41−44]

$$\frac{1}{T_1} = Kn[J(\omega_H - \omega_C) + 3J(\omega_C) + 6J(\omega_H + \omega_C)] \tag{3}$$

$$\mathrm{NOE} = 1 + \frac{\gamma_H}{\gamma_C}\left[\frac{6J(\omega_H + \omega_C) - J(\omega_H - \omega_C)}{J(\omega_H - \omega_C) + 3J(\omega_C) + 6J(\omega_H + \omega_C)}\right] \tag{4}$$

In these expressions, $\omega_H/2\pi$ and $\omega_C/2\pi$ are Larmor frequencies of ^{1}H and ^{13}C nuclei, respectively, n is the number of protons attached to the ^{13}C nuclei of interest ($n = 2$ for methylene carbons), γ_H and γ_C are the gyromagnetic ratios of ^{1}H and ^{13}C, and K is a constant which depends on the average C−H internuclear distance (equal to 2.29×10^9 s^{-2} for methylene units).[45]

For deuterium nuclei, relaxation is dominated by the electric quadrupole coupling and has the following relationship to the reorientation of a C−D bond:[41−44]

$$\frac{1}{T_1} = \frac{3}{10}\pi^2\left(\frac{e^2qQ}{h}\right)^2[J(\omega_D) + 4J(2\omega_D)] \tag{5}$$

Here $\omega_D/2\pi$ is the Larmor frequency of deuterium. The deuterium quadrupole coupling constant e^2qQ/h was taken as 172 and 190 kHz for the backbone and side group deuterons, respectively.[43,46,47]

Correlation Function and Correlation Time. The correlation function $G(t)$ is not directly observable in the NMR measurements. We proceed by assuming a particular functional form for it and then optimizing the fit parameters by comparison with the experimental data. The modified KWW function was shown to give an excellent fit to the experimental data for several polymers over wide temperature range.[48−50] It is composed of an exponential term characterizing the fast librational motion and a stretched exponential term representing the slower segmental motion.

$$G(t) = a_{lib}\exp\left(-\frac{t}{\tau_{lib}}\right) + (1 - a_{lib})\exp\left[-\left(\frac{t}{\tau_{seg}}\right)^{\beta}\right] \tag{6}$$

Here a_{lib} and τ_{lib} characterize the amplitude and relaxation time for librational motion. Fits to the experimental data were insensitive to τ_{lib}, and this parameter was set equal to 1 ps. τ_{seg} and β describe a characteristic segmental relaxation time as well as the distribution of times associated with it. We assume that τ_{seg} follows a VTF temperature dependence.[51,52]

$$\log\left(\frac{\tau_{seg}}{\tau_\infty}\right) = \frac{B}{T - T_0} \tag{7}$$

where τ_∞, B, and T_0 are constants for a given component in a particular sample. Usually we are interested in the correlation time for segmental dynamics $\tau_{seg,c}$, which is defined as the integral of the segmental portion of the correlation function:

$$\tau_{seg,c} = \frac{\tau_{seg}}{\beta}\Gamma\left(\frac{1}{\beta}\right) \tag{8}$$

Results

Figures 1−2 show the ^{13}C T_1 and NOE values measured at two different magnetic fields for the C1 carbons of pure PI and the isoprene segments in the four SISI copolymers. The data for pure PI in Figure 2 comes from ref 16. Note that the T_1 minimum moves successively to higher temperatures as the fraction of styrene units increases. Since the T_1 minimum indicates the temperature at which the segmental dynamics occur on roughly a 1 ns time scale, this qualitatively indicates that the isoprene segmental dynamics are slowed down by surrounding styrene units. For SISI80, the T_1 minimum shifts to higher temperatures by about 70 K as compared with pure PI. NOE data exhibit the same variation with composition, shifting to higher temperatures with increasing styrene content. For all samples, the C4 carbons have higher T_1 values than C1 carbons but a very similar temperature dependence, and the T_1 minimum positions only differ by about 5 K. Thus, the two backbone carbons have very similar dynamics. The data for C4 carbons can be found in the Supporting Information.

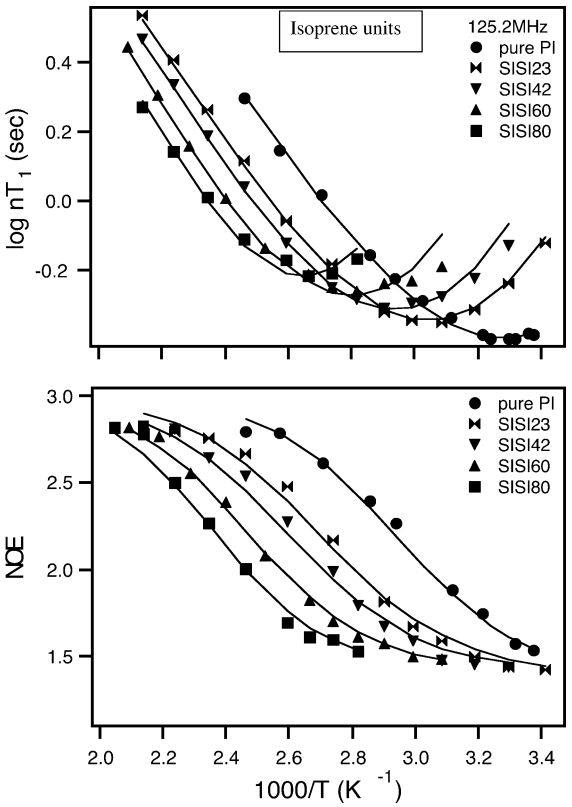

Figure 2. ^{13}C NMR relaxation time measurements for C1 carbons in pure PI and isoprene segments of the four tetrablock copolymers at 125.2 MHz. Solid lines are the fit results using the mKWW autocorrelation function and VTF temperature dependence.

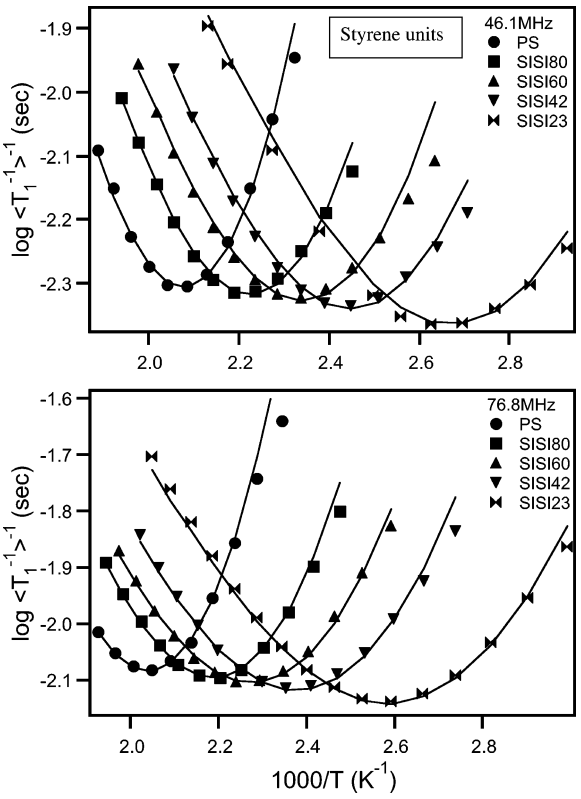

Figure 3. ^{2}H NMR relaxation time measurements for per-deuterated pure PS and styrene segments of the four tetrablock copolymers at 46.1 and 76.8 MHz. The rate averaged T_1 values for all the backbone and phenyl ring deuterons are presented. Solid lines are the fit results using the mKWW autocorrelation function and VTF temperature dependence.

Figure 3 shows the rate-averaged ^{2}H T_1 values measured at two different magnetic fields for all deuterons of pure PS and the styrene segments in the tetrablock copolymers. Clearly, the T_1 minima at both frequencies move toward lower temperatures with increasing isoprene content, qualitatively indicating that the styrene segmental dynamics become faster due to the presence of isoprene segments. For SISI23, which has the highest isoprene content, the T_1 minimum decreases by about 105 K compared to the T_1 minimum of pure PS, indicating a very large change in terms of segmental dynamics.

Superposition of the Experimental Data. A model independent way of examining the effect of mixing upon segmental dynamics is to directly superpose the experimental data using temperature shifts.[53] As shown in Figure 4, we found that temperature shifts (not shifts in terms of 1000/T) produced a reasonable master curve for pure PS and styrene segments in all the tetrablock samples. Small vertical shifts were needed to superpose the T_1 data (see Table 2).

Analogous superposition curves at 125.2 MHz for ^{13}C T_1 and NOE of pure PI and isoprene segments in tetrablock copolymers are presented in Figure 5. (The superposition curves at 75.6 MHz are comparable but are not shown here.) Here the superposition for the isoprene segments is not quite as good as that for the styrene segments. Pure PI has a slightly narrower T_1 curve, and the isoprene segments in SISI80 have a broader T_1 curve compared to other tetrablock samples. For SISI tetrablock copolymers, there are a few isoprene and styrene units immediately located at each side of each junction point whose dynamics are significantly

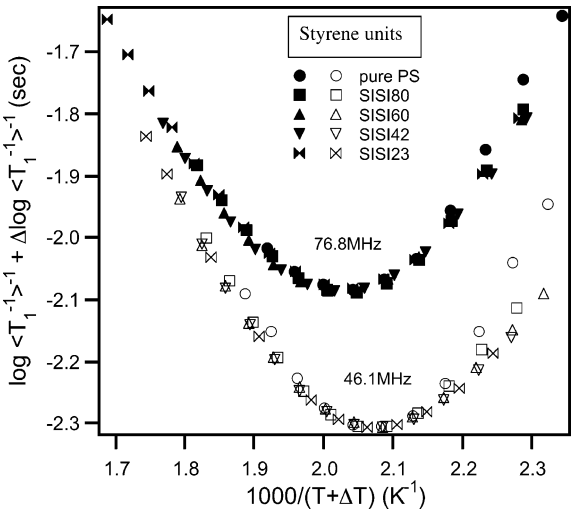

Figure 4. Superposition of the rate averaged T_1 data for pure PS and four tetrablock copolymers. A single temperature and vertical shift suffice to superpose the data at 76.8 and 46.1 MHz simultaneously for a given composition copolymer.

influenced by the other component. It is probable that this influence is much stronger than that from neighboring chains in the case of simple mixing. In SISI80, a significant fraction of the isoprene units are very near a junction point. We propose that this "junction effect" causes a broader distribution of isoprene segmental relaxation times for SISI80. Results discussed below support this hypothesis.

All shift parameters used to construct Figures 4 and 5 are listed in Table 2. While the superposition curves

Table 2. Horizontal and Vertical Shifts Needed To Superpose the Experimental Data of Tetrablock Copolymers onto Those of Pure Homopolymers

components	samples	$\Delta \log(nT_1)$ (s)	ΔT (K)	ΔT_0 (K)[a]
Isoprene	SISI23	−0.04	−28	−28
	SISI42	−0.08	−40	−40
	SISI60	−0.11	−54	−54
	SISI80	−0.18	−72	−68
d_8-Styrene	SISI80	0.009	31	33
	SISI60	0.018	52	56
	SISI42	0.029	71	76
	SISI23	0.058	104	106

[a] From fits in Table 3.

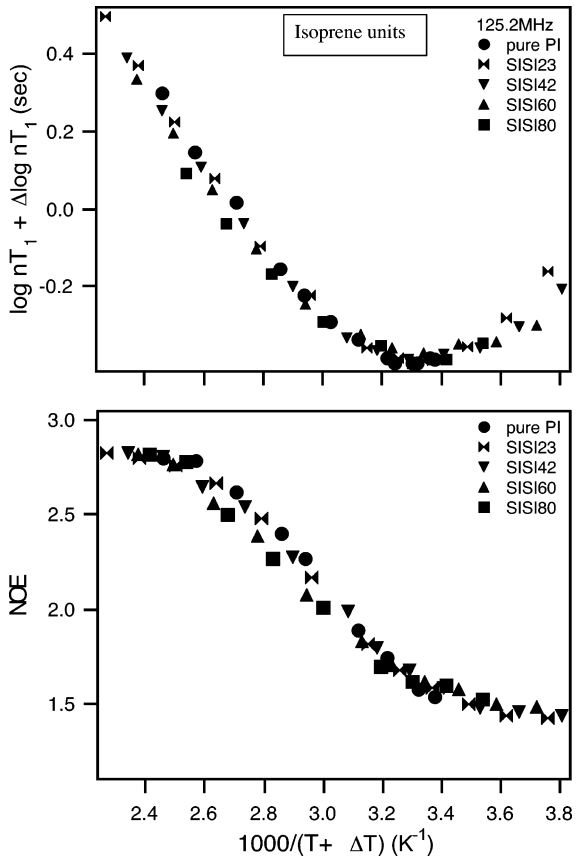

Figure 5. Superposition of T_1 and NOE data for pure PI and four tetrablock copolymers. A single temperature and vertical shift suffice to superpose the data for two methylene carbons at 76.8 and 46.1 MHz simultaneously for a given composition copolymer. Only the data of carbon 1 are shown here.

are not perfect, they are adequate to provide a model-independent check on the fitting results obtained below. A strong indication that these shifts are meaningful is the fact that the same temperature and vertical shifts sufficed to superpose both the T_1 and NOE data at two different fields (NOE is only available for the isoprene units). In addition, the same shifts superposed the data from the C4 carbon of isoprene units (not shown here).

Fits to mKWW and VTF Functions. Although the superposition procedure provides some information about the effects of mixing on the component segmental dynamics, fitting the experimental data to a model correlation function allows us to extract the segmental relaxation times and have a more quantitative description of the experimental results. As we show below, this model-dependent fitting procedure produced results in good agreement with the model-independent shifting methods. Since we found in a previous study[49] that the mKWW function (eq 6) provides an excellent fit to NMR relaxation time data, we employed it here in combination with the assumption of VTF temperature dependence (eq 7).

Fitting was performed individually on the experimental data set for each nucleus in each sample using eqs 1−7. For each of the two carbons of isoprene units, ^{13}C T_1 and NOE at both frequencies were fitted simultaneously. In this procedure, there are five unknown parameters: a_{lib}, β, τ_∞, B, and T_0. Because of the relatively small range of correlation times sampled in these NMR measurements, B and T_0 are highly correlated with each other, and one of these two parameters needed to be constrained to produce reasonable trends in terms of mixing. As detailed in the rest of this paragraph, a variety of fitting procedures were employed, all of which yield the same values of the segmental correlation times within 0.1 decade. According to previous work on PI/PVE blends,[16] T_0 closely tracks the variation of the T_1 minimum temperature when constraining B to a constant value. Here we chose to constrain T_0 to follow the T_1 minimum temperature for all samples with the exception of SISI80, for which the T_1 minimum is blurred out by the junction effect. (For SISI80, ΔT_0 was allowed to deviate slightly from ΔT_1. For this sample, a bimodal distribution of segmental relaxation times fits the isoprene data better than the unimodal distribution (eq 6); these results are not presented here.) As the styrene fraction increases, we needed to either decrease β or increase a_{lib}. In Table 3, we list only the parameters obtained by the second procedure, but the segmental correlation times from these two fitting procedures agree with each other within 0.1 decade. As shown by the solid lines in Figures 1−3, the parameters in Table 3 yielded good fits to the experimental data, even though there is some deviation for the samples with very short isoprene segments (strong junction effect). If we constrain B and allow T_0 to be a free fit parameter, the segmental correlation times differ by less than 0.1 decade.

A similar fitting procedure was used for the T_1 data of styrene units, except that T_0 was not constrained to track the T_1 minimum. Again there are two ways to fit the data: constrain a_{lib} or constrain β. Since the proportion of librational motion was expected to be independent of the environment of molecules,[54] and this approach yielded excellent fits to the experimental data, we chose to constrain a_{lib} to its pure homopolymer value (0.23). For most samples, the difference between the segmental correlation times extracted from these two methods is less than 0.2 decade. Only for SISI23, at the lowest temperature of our experiments, is there a larger difference (0.3 decade). For both components, there is substantial uncertainty (±0.1) in the fitted values of β.

Segmental Correlation Times. From the fit parameters in Table 3, the segmental correlation times of isoprene and styrene segments were calculated using eq 8. The resulting curves are plotted in Figure 6. As expected, the correlation times of isoprene segments at a given temperature increase as the styrene fraction increases, and this effect is more pronounced at low temperatures. On the other hand, the segmental dynamics of styrene become faster with increasing isoprene fraction. Though the qualitative shapes of the correlation time curves are the same for isoprene and styrene segments, the slopes are steeper for styrene segments, indicating a higher apparent activation en-

Table 3. Best Fit Parameters for Segmental Dynamics of Isoprene and Styrene Segments in Tetrablock Copolymers and Homopolymers

		samples					
fit parameters		pure PI	SISI23	SISI42	SISI60	SISI80	pure PS
Isoprene							
C_1	β	0.52	0.47	0.45	0.44	0.45	
	τ_∞ (ps)	0.11	0.11	0.094	0.075	0.081	
	T_0 (K)	158	185	197	211	226	
	B (K)	557	545	547	578	589	
	A_{lib}	0.30	0.32	0.35	0.39	0.52	
C_4	β	0.50	0.45	0.42	0.42	0.42	
	τ_∞ (ps)	0.13	0.10	0.085	0.082	0.10	
	T_0 (K)	162	190	202	216	230	
	B (K)	503	507	507	521	517	
	A_{lib}	0.33	0.36	0.38	0.43	0.53	
d_8-Styrene	β		0.54	0.51	0.50	0.48	0.47
	τ_∞ (ps)		0.98	0.78	0.71	0.52	0.30
	T_0 (K)		211	241	261	284	317
	B (K)		526	540	542	577	614
	A_{lib}		0.23	0.23	0.23	0.23	0.23

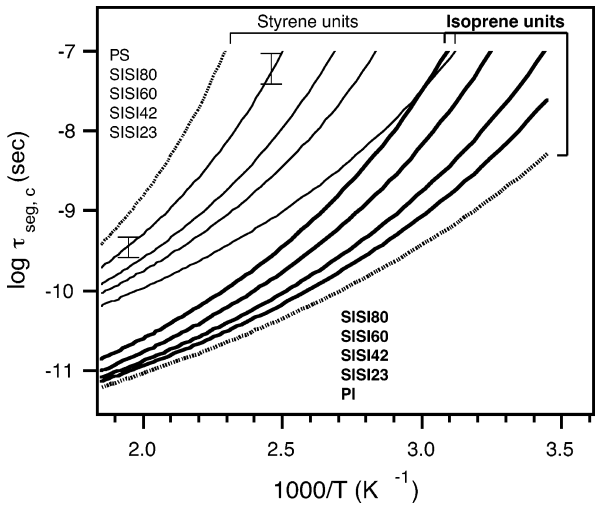

Figure 6. Segmental correlation times for two pure homopolymers and four tetrablock copolymers calculated using the fit parameters in Table 3. For isoprene segments, the plotted lines represent the average behavior of the two methylene carbons. A temperature shift of 9 K to higher temperatures was made to pure PI to account for the molecular weight dependence of T_g (as explained in the text). Error bars reflect the uncertainty associated with the fitting procedures.

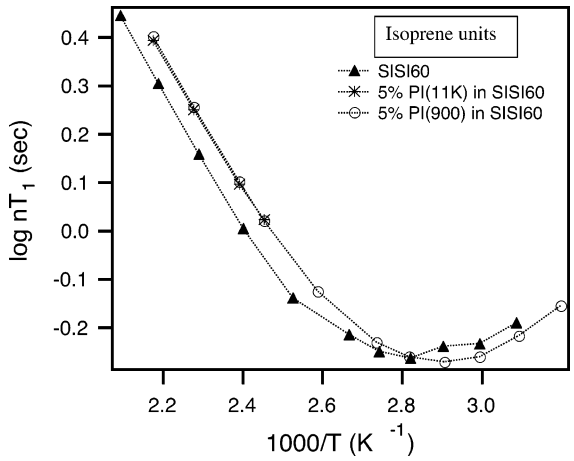

Figure 7. ^{13}C NMR relaxation time measurements for C1 carbons in isoprene segments of SISI60 and two PI tracers (PI-1K and PI-11K) in SISI60 matrix at 125.2 MHz. The dotted lines guide the eye.

ergy for this component in a given copolymer at a given temperature. Also, the change in dynamics with composition is larger for styrene segments than for isoprene segments.

Because the correlation times of the two different carbons in isoprene units are very similar at any temperature within the range of these experiments, they were averaged, and the average values are used for further discussion. The similarity of the correlation times for these two carbons is expected and is one indication of the robustness of the fitting procedure. Another indication is the excellent agreement between the shifts in T_0 and the temperature shifts deduced from the superposition procedure for styrene segments (see comparison in Table 3). The uncertainty in the reported correlation times, as reflected by different fitting procedures, is shown by representative error bars in the figure. In constructing this figure, the segmental correlation times of pure PI ($M_n = 1350$) have been shifted to high temperature by 9 K to account for the T_g difference, so now the curve in Figure 6 corresponds to the segmental correlation time of a higher molecular weight PI ($M_n \approx 11\,000$).

Segmental Dynamics of Tracers in Tetrablock Matrix. ^{13}C labeling enables us to measure the segmental dynamics of a low-concentration PI tracer in a tetrablock matrix. 5% PI-1K and PI-11K homopolymers were put into SISI60 as tracers, and the segmental dynamics of these tracers were measured. Because both PI tracers are 66% ^{13}C labeled in C1 position, about 90% of the C1 NMR resonance signals come from the tracers, and only 10% comes from the isoprene segments of SISI60 matrix. As an approximation, we neglect the contribution from the matrix and take the measured values as the T_1 of PI tracers. Figure 7 shows the T_1 for the isoprene segments (C1 carbon) in the two 5% PI/SISI60 blends plotted with the T_1 values for the isoprene segments in SISI60. Here only four data points were obtained for high molecular weight tracer PI-11K because of phase separation at low temperatures. The two tracers show about the same T_1 values, and both superpose well with the T_1 curve of isoprene segments in the SISI60 matrix after shifting both sets of tracer data to higher temperature by 9 K (not shown). While we do not attempt to quantitatively explain the 9 K shift here, this indicates that the segmental dynamics of PI tracers are nearly identical to (but slightly faster than) those of isoprene segments in tetrablock copolymers.

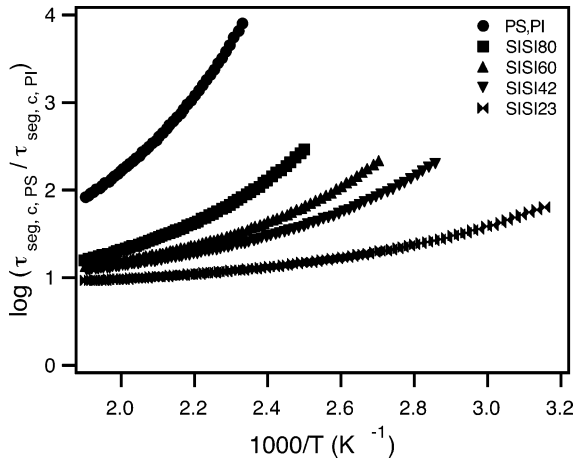

Figure 8. Ratios of segmental correlation times of styrene and isoprene segments in pure melts (upper curve) and tetrablock copolymers (lower four curves), calculated from fits shown in Figure 6.

Discussion

Dynamic Heterogeneity. Lodge and co-workers investigated the tracer diffusion of a PS homopolymer, a PI homopolymer, and a SI diblock copolymer in SISI tetrablock matrices as a function of temperature and matrix composition. Remarkably, the friction factors of PS, PI, and SI in a given tetrablock matrix are quite similar (within a factor of 2−3) and also nearly equal to the friction factor of the matrix itself.[31] These results indicate that the tracer diffusion effectively senses a quite homogeneous dynamic environment.

From Figure 6 we can clearly see that isoprene and styrene segments in the tetrablock copolymers have very different segmental dynamics and very different apparent activation energies. If we plot the ratio of segmental correlation times of styrene and isoprene segments vs temperature (as shown in Figure 8), this difference is much more apparent. For any given sample at any temperature, the dynamics of styrene segments are always slower than that of isoprene segments, and the dynamic difference between them grows larger as the temperature is lowered. We ascribe this dynamic heterogeneity to the huge dynamic difference between PI and PS homopolymers ($\Delta T_g \approx 170$ K).

If we extrapolate the curves in Figure 6 to longer time scales, the difference between the dynamics of the styrene and isoprene segments at the copolymer T_g is up to 7 orders of magnitude. Using these extrapolations, we defined an effective T_g for one component in the tetrablock copolymers as that temperature at which $\tau_{seg,c}$ is predicted to be 1 s. The difference in effective T_g of the two components ranges from 20 K for SISI23 to 80 K for SISI80. This suggests that the tetrablock samples should have very broad glass transitions. This deduction is strongly supported by the fact that the glass transition temperatures of these tetrablock samples were not readily measurable by DSC.[30] Preliminary results from lower temperature experiments by Fytas and co-workers are in reasonable agreement with our extrapolations.[55]

A central question is how the very heterogeneous segmental dynamics in the SISI tetrablocks give rise to the homogeneous global dynamics discussed above. We will focus on this issue in a future publication.[33]

Intrinsic Mobility Difference. Another interesting phenomenon in Figure 8 is that at very high temperatures the results for all four tetrablock samples seem to converge to a common value $\log \tau_{seg,c,PS}/\tau_{seg,c,PI} = 1.0-1.2$. This difference should be attributed to either the different intrinsic mobilities of the two kinds of chains or a local composition effect, or both. From Figure 6 we can see that, at the highest temperature of our experiments, the dynamic differences for each component caused by the composition variation are no more than 0.5 decade and diminish rapidly with increasing temperature. Thus, we interpret the 1 decade dynamic difference in Figure 8 at high temperatures as the intrinsic mobility difference due to differences in the molecular structure and intramolecular potentials for isoprene and styrene segments.[56] Qualitatively, the faster dynamics observed for isoprene segments is reasonable given the absence of large side group. If this reasoning is correct, then a similar intrinsic mobility difference should be observed for pure PI and PS in dilute solution with low molecular weight solvents. Indeed, this is the case. The segmental dynamics of pure PI and PS have been measured in a number of solvents.[54,57] In *cis*-decalin the segmental dynamics of PI is 0.9 decade faster than that of PS at 500 K (estimated from measurements done at slightly lower temperatures). This agreement strongly supports our suggestion here. A similarly strong correlation between dilute solution data and high-temperature polymer mixture data was obtained for the PI/PVE system.[16]

Junction Effect on Segmental Dynamics. As mentioned above, a unimodal distribution of segmental relaxation times is not able to quantitatively describe the T_1. values of isoprene segments in SISI80. This might be due to the junction effect on such short isoprene chains (16 repeat units on average). In the SISI tetrablock copolymers, a few isoprene units immediately next to a junction point should have much slower dynamics than the isoprene units away from the junction points. This is likely to be the reason why a unimodal distribution of segmental relaxation times does not adequately fit the data.

In Figure 7, we showed that PI homopolymer tracers in SISI60 have faster segmental dynamics than the average isoprene segments in the copolymer matrix. This is consistent with our hypothesis of a junction effect on isoprene segments. That is, we assume that the chemical attachment of a styrene chain (high T_g component) to the isoprene chain makes the isoprene segments of the matrix have slower dynamics on average than that of the free PI tracer. The junction effect on styrene segments presumably also influences our experimental results, although here the impact is apparently not as strong.

Though the existence of a junction effect is clear, it is difficult to quantify the number of repeat units near a junction that are affected by it. It is reasonable to think that the junction effect in block copolymers is similar to the chain end effect in homopolymers. Under this assumption molecular dynamics simulations provide some indications about how strong the effect is. Lyulin and co-workers[58] showed that PS chain ends influence the mobility of only a few neighboring monomers (3−5 nearest neighbors), both in the backbone and in the aromatic side groups. Faller and co-workers[59] reported that for PI there are three monomers at each chain end that have a discernible difference from the central monomers in terms of the relaxation times of C−H vector reorientation.

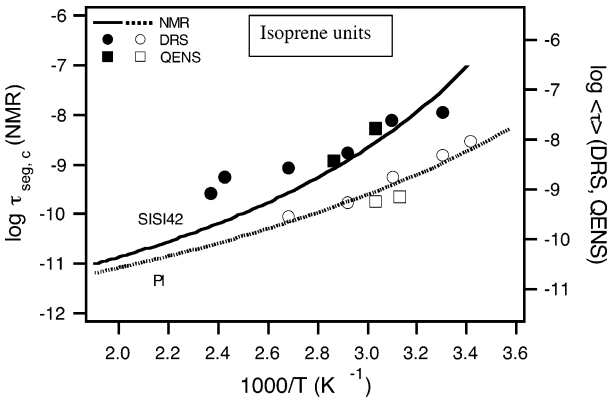

Figure 9. Comparison of segmental correlation times for pure PI and isoprene segments in SISI42 with previous work on the same samples using quasi-elastic neutron scattering (QENS) and depolarized Rayleigh light scattering (DRS).[32]

Comparison with Other Work on SISI. Fytas and co-workers[32] have used quasi-elastic neutron scattering (QENS) and dynamic light scattering to investigate the segmental relaxation of isoprene segments in SISI42 and pure PI. The comparison between our results and theirs is shown in Figure 9. Note that there is a half decade relative vertical shift between the two sets of data; this is not surprising since NMR, QENS, and dynamic light scattering measure different observables and may account for segmental dynamics at slightly different length scales. For pure PI, the two sets of data agree very well with each other. For isoprene units in SISI42, there is some inconsistency among the different techniques at high temperatures but good agreement at lower temperatures.

Concluding Remarks

We have investigated the segmental dynamics of isoprene and styrene segments in four SISI tetrablock copolymers using ^{13}C and ^{2}H NMR at two magnetic fields. The mKWW orientation autocorrelation function combined with a VTF temperature dependence was employed to extract segmental correlation times. The trends of correlation time variation with composition obtained in this way agree well with those inferred from a model-independent superposition approach.

The SISI tetrablocks show large differences between the segmental dynamics of the two components and the dynamic difference becomes larger toward lower temperatures. At temperatures far above T_g, the segmental dynamics of styrene segments are slower than that of isoprene segments by about 1 decade. This can be attributed to an intrinsic mobility difference and is in quantitative agreement with measurements of each chain individually as a dilute component in a common solvent. The segmental dynamics of a 5% PI tracer (either 11 or 1 K) are similar to but slightly faster than that of isoprene segments in SISI. The slight difference is consistent with a junction effect, which strongly modifies the segmental dynamics of segments near the junction point.

In contrast to the very heterogeneous dynamics found on the segmental level, the global dynamics inferred from tracer diffusion are homogeneous.[31] The relationship between the segmental and global dynamics in SISI will be addressed in a future publication.[33]

Acknowledgment. This research was partly supported by American Chemical Society, the Petroleum Research Fund (PRF 35134-AC), and the National Science Foundation (DMR-0099849). We thank Prof. Tim Lodge for helpful discussions and Dr. Charles Fry and Marv Kontney for their technical support. Measurements were performed at the Instrument Center of the Department of Chemistry, University of Wisconsin−Madison, supported by NSF CHE-9508244 and CHE-9629688. The fitting work was done at the computer center of the Department of Chemistry, University of Wisconsin−Madison, supported by NSF CHE-0091916.

Supporting Information Available: Figures showing the ^{13}C T_1 and NOE data measured at two different magnetic fields for the C4 carbons of pure PI and the isoprene segments in the four SISI tetrablock copolymers. This material is available free of charge via the Internet at http://pubs.acs.org.

References and Notes

(1) Chung, G. C.; Kornfield, J. A.; Smith, S. D. *Macromolecules* **1994**, *27*, 964−973.
(2) Kumar, S. K.; Colby, R. H.; Anastasiadis, S. H.; Fytas, G. *J. Chem. Phys.* **1996**, *105*, 3777−3788.
(3) Yang, X.; Halasa, A.; Hsu, W. L.; Wang, S. Q. *Macromolecules* **2001**, *34*, 8532−8540.
(4) Roland, C. M.; Ngai, K. L. *Macromolecules* **1991**, *24*, 2261−2265.
(5) Colby, R. H. *Polymer* **1989**, *30*, 1275−1278.
(6) Trask, C. A.; Roland, C. M. *Macromolecules* **1989**, *22*, 256−261.
(7) Miller, J. B.; McGrath, K. J.; Roland, C. M.; Trask, C. A.; Garroway, A. N. *Macromolecules* **1990**, *23*, 4543−4547.
(8) Alegria, A.; Colmenero, J.; Ngai, K. L.; Roland, C. M. *Macromolecules* **1994**, *27*, 4486-4492.
(9) Ngai, K. L.; Roland, C. M. *Macromolecules* **1995**, *28*, 4033−4035.
(10) Chung, G. C.; Kornfield, J. A.; Smith, S. D. *Macromolecules* **1994**, *27*, 5729−5741.
(11) Alvarez, F.; Alegria, A.; Colmenero, J. *Macromolecules* **1997**, *30*, 597−604.
(12) Arbe, A.; Alegria, A.; Colmenero, J.; Hoffmann, S.; Willner, L.; Richter, D. *Macromolecules* **1999**, *32*, 7572−7581.
(13) Hoffmann, S.; Willner, L.; Richter, D.; Arbe, A.; Colmenero, J.; Farago, B. *Phys. Rev. Lett.* **2000**, *85*, 772−775.
(14) Adams, S.; Adolf, D. B. *Macromolecules* **1999**, *32*, 3136−3145.
(15) Doxastakis, M.; Kitsiou, M.; Fytas, G.; Theodorou, D. N.; Hadjichristidis, N.; Meier, G.; Frick, B. *J. Chem. Phys.* **2000**, *112*, 8687−8694.
(16) Min, B.; Qiu, X. H.; Ediger, M. D.; Pitsikalis, M.; Hadjichristidis, N. *Macromolecules* **2001**, *34*, 4466−4475.
(17) Roland, C. M.; Ngai, K. L. *Macromolecules* **1992**, *25*, 363−367.
(18) Zetsche, A.; Fischer, E. W. *Acta Polym.* **1994**, *45*, 168−175.
(19) Pathak, J. A.; Colby, R. H.; Floudas, G.; Jerome, R. *Macromolecules* **1999**, *32*, 2553−2561.
(20) Cendoya, I.; Alegria, A.; Alberdi, J. M.; Colmenero, J.; Grimm, H.; Richter, D.; Frick, B. *Macromolecules* **1999**, *32*, 4065−4078.
(21) Lartigue, C.; Guillermo, A.; Cohen-Addad, J. P. *J. Polym. Sci., Polym. Phys. Ed.* **1997**, *35*, 1095−1105.
(22) Schantz, S. *Macromolecules* **1997**, *30*, 1419−1425.
(23) Dionisio, M.; Fernandes, A. C.; Mano, J. F.; Correia, N. T.; Sousa, R. C. *Macromolecules* **2000**, *33*, 1002−1011.
(24) Lutz, T. R.; He, Y.; Ediger, M. D.; Cao, H.; Lin, G.; Jones, A. A. *Macromolecules* **2003**, *36*, 1724−1730.
(25) Chin, Y. H.; Zhang, C.; Wang, P.; Inglefield, P. T.; Jones, A. A.; Kambour, R. P.; Bendler, J. T.; White, D. M. *Macromolecules* **1992**, *25*, 3031−3038.
(26) Chin, Y. H.; Inglefield, P. T.; Jones, A. A. *Macromolecules* **1993**, *26*, 5372−5378.
(27) Ngai, K. L.; Roland, C. M.; O'Reilly, J. M.; Sedita, J. S. *Macromolecules* **1992**, *25*, 3906−3909.
(28) Kim, E.; Kramer, E. J.; Osby, J. O. *Macromolecules* **1995**, *28*, 1979−1989.
(29) Urakawa, O.; Fuse, Y.; Hori, H.; Tran-Cong, Q.; Yano, O. *Polymer* **2001**, *42*, 765−773.
(30) Chapman, B. R.; Hamersky, M. W.; Milhaupt, J. M.; Kostelecky, C.; Lodge, T. P.; von Meerwall, E. D.; Smith, S. D. *Macromolecules* **1998**, *31*, 4562−4573.

(31) Milhaupt, J. M.; Chapman, B. R.; Lodge, T. P.; Smith, S. D. *J. Polym. Sci., Polym. Phys. Ed.* **1998**, *36*, 3079−3086.
(32) Doxastakis, M.; Chrissopoulou, K.; Aouadi, A.; Frick, B.; Lodge, T. P.; Fytas, G. *J. Chem. Phys.* **2002**, *116*, 4707−4714.
(33) He, Y.; Lutz, T. R.; Ediger, M. D.; Lodge, T. P., submitted to *Macromolecules*.
(34) Rizos, A. K.; Fytas, G.; Semenov, A. N. *J. Chem. Phys.* **1995**, *102*, 6931−6940.
(35) Se, K.; Takayanagi, O.; Adachi, K. *Macromolecules* **1997**, *30*, 4877−4881.
(36) He, Y.; Lutz, T. R.; Ediger, M. D.; Pitsikalis, M.; Hadjichristidis, N., manuscript in preparation.
(37) Kaplan, M. L.; Bovey, F. A.; Cheng, H. N. *Anal. Chem.* **1975**, *47*, 1703−1705.
(38) Choi, S.; Lee, K. M.; Han, C. D.; Sota, N.; Hashimoto, T. *Macromolecules* **2003**, *36*, 793−803.
(39) Chiantore, O.; Guaita, M.; Lazzari, M.; Hadjichristidis, N.; Pitsikalis, M. *Polym. Degrad. Stab.* **1995**, *49*, 385−392.
(40) Bovey, F. A.; Mirau, P. A. *NMR of Polymers*; Academic Press: San Diego, CA, 1996.
(41) Abragam, A. *The Principle of Nuclear Magnetism;* Clarendon Press: Oxford, 1961; Chaper VIII.
(42) Lyerla, J. R.; Levy, G. C. *Top. Carbon-13 NMR Spectrosc.* **1974**, *1*, 79.
(43) Heatley, F. *Prog. Nucl. Magn. Reson. Spectrosc.* **1979**, *13*, 47−85 and references therein.
(44) Heatley, F. *Annu. Rep. NMR Spectrosc.* **1986**, *17*, 179−230 and references therein.
(45) Gisser, D. J.; Glowinkowski, S.; Ediger, M. D. *Macromolecules* **1991**, *24*, 4270−4277.
(46) Loewenstein, A. *Advances in Nuclear Quadrupole Resonance;* John Wiley & Sons: London, 1983; Vol. 5.
(47) Lucken, E. A. C. *Nuclear Quadrupole Coupling Constants;* Academic Press: London, 1969.
(48) Bandis, A.; Wen, W. Y.; Jones, E. B.; Kaskan, P.; Jones, A. A.; Inglefield, P. T.; Bendler, J. T. *J. Polym. Sci., Polym. Phys. Ed.* **1994**, *32*, 1707−1717.
(49) Moe, N. E.; Qiu, X. H.; Ediger, M. D. *Macromolecules* **2000**, *33*, 2145−2152.
(50) Qiu, X. H.; Moe, N. E.; Ediger, M. D.; Fetters, L. J. *J. Chem. Phys.* **2000**, *113*, 2918−2926.
(51) Angell, C. A. *Polymer* **1997**, *38*, 6261−6266.
(52) Tammann, G.; Hesse, W. *Z. Anorg. Allg. Chem.* **1926**, *156*, 245.
(53) Laupretre, F.; Monnerie, L.; Roovers, *J. PMSE Prepr.* **2000**, *82*, 154.
(54) Zhu, W.; Ediger, M. D. *Macromolecules* **1997**, *30*, 1205−1210.
(55) Fytas, G. Personal communication, 2002.
(56) This interpretation is consistent with the τ_∞ values reported for each tetrablock in Table 3.
(57) Glowinkowski, S.; Gisser, D. J.; Ediger, M. D. *Macromolecules* **1990**, *23*, 3520−3530.
(58) Lyulin, A. V.; Michels, A. J. *Macromolecules* **2002**, *35*, 1463−1472.
(59) Faller, R.; Muller-Plathe, F.; Doxastakis, M.; Theodorou, D. *Macromolecules* **2001**, *34*, 1436−1448.

MA030350G